Mater. Res. Soc. Symp. Proc. Vol. 1083 © 2008 Materials Research Society 1083-R04-11

Numerical Modeling of Electrothermal Effects in Silicon Nanowires

Cicek Boztug, Gokhan Bakan, Mustafa Akbulut, Ali Gokirmak, and Helena Silva
Department of Electrical and Computer Engineering, University of Connecticut, Storrs, CT, 06269

Abstract

Asymmetric melting was observed in electrically pulsed n-type (phosphorus) nanocrystalline silicon (nc-Si) wires fabricated lithographically. Scanning electron microscope (SEM) images taken from the pulsed wires showed that melting initiates from the ground terminal end of the wires instead of the center as initially expected. Asymmetry in the temperature profile is caused by heat exchanged between charge carriers and phonons when an electrical current is passed along a temperature gradient. This effect is known as Thomson effect, a thermoelectric heat transfer mechanism. One dimensional (1D) time dependent heat diffusion equation including Thomson heat term was solved to model the temperature profile on our structures. The modeling results show that Thomson effect introduces significant shifts in the temperature distribution. The effect of Thomson heat is modeled for various electrical pulse conditions and wires dimensions. Our results indicate that Thomson effect is significant in small scale electronic devices operating under high current densities.

Introduction

Heat transfer is a critical mechanism in devices that utilize coupled electrical and thermal effects such as thermoelectric devices and phase change memory devices, as well as in conventional electronics. In thermoelectric coolers an electrical current is passed through the junction between two dissimilar materials. Although the cooling occurs at the junction due to the Peltier effect [1], hotspots originated by the applied current appear on both materials. In these devices the location of the hotspot affects the cooling efficiency of the junction and the Thomson effect can be utilized to improve performance [2]. Programming of phase change memory cells is based on Joule heating due to a short current pulse applied through the cell. Thermal transport during the pulse has to be modeled accurately since it directly affects the programming characteristics of the cell [3]. Furthermore, investigation of heat transport at small scales is crucial to understand hotspots formed in electronic devices and integrated circuits which lead to reliability and performance issues [4]. Thomson effect has been observed before in larger scale silicon structures under high current densities [5, 6].

In order to study the Thomson effect on the temperature distribution of electrically pulsed n-type nc-Si sub-μm wires the 1D time dependent heat diffusion equation is solved numerically including heat conduction along the wires and to the substrate, Joule heat and Thomson heat.

Fabrication and SEM characterization of pulsed nanocrystalline Si wires

Wires with various lengths (L ~ 1-5.5 μm) and widths (W ~ 200 - 450 nm) with large contact pads were defined on a 75 nm thick n-type (phosphorus) nc-Si film on SiO_2, and etched using reactive ion etching (RIE). The resistivity of the films from which the wires were fabricated is about $3x10^{-4}$ Ω.m as determined by four-point probe measurements. The doping density is on the order of 10^{20} cm^{-3} as determined by Auger analysis. Underlying SiO_2 was partially etched, creating a wire bridge between the electrode pads as shown in Figure 1(a). The large area pads are used to probe the wires, and to apply 1 μs voltage pulse with amplitude

between 30-40 V. The SEM image of a pulsed wire [Fig. 1(b)] shows a significant texture change in one end of the wire indicating asymmetric heating and melting. Current-voltage (I-V) measurements are performed before and after the electrical pulse. Figure 1(c) shows the I-V curves for a 2.5 µm wire before and after the electrical pulse. The highly linear I-Vs indicate ohmic contacts between the tungsten probes and the heavily doped silicon pads suggesting that contacts do not play a role in the asymmetrical heating. This hypothesis is further tested by reversing the polarity of the pulse and by electrical stress of numerous different wires. It is observed that the melting consistently initiates from the low voltage terminal end which indicates that the asymmetry is not a contact effect. Since the structure formed by the pads and the wire is approximately symmetric (within fabrication process variations), it was initially expected that the Joule heated wires would reach their maximum temperature at the center which would cause melting to start from center and symmetrically spread to the ends. After the observation of the asymmetric melting of the structures towards the low voltage terminal end, the 1D time dependent heat diffusion equation was solved numerically to correlate our experimental observations with theory.

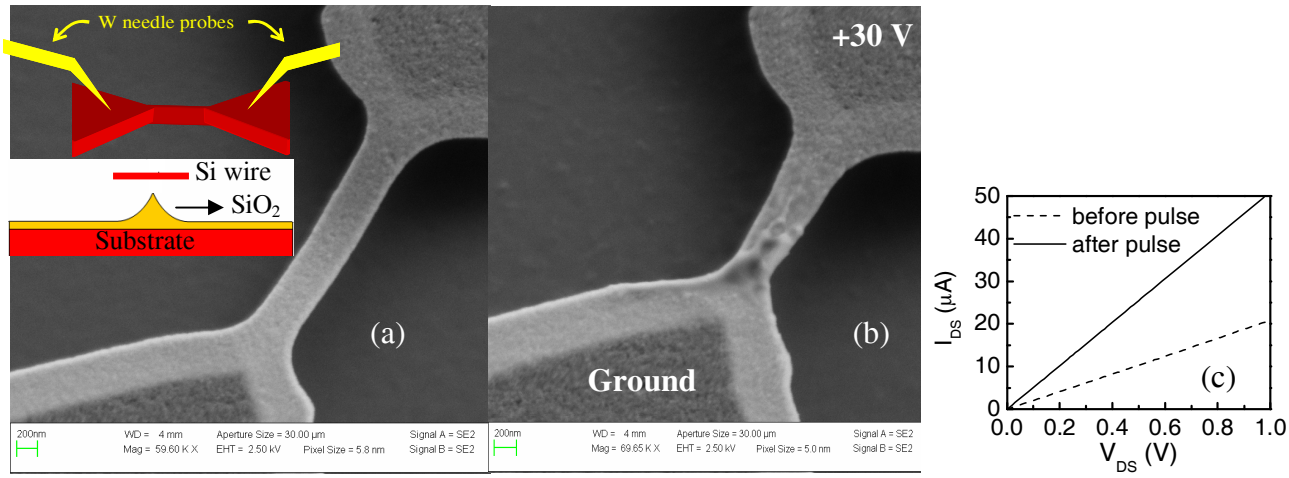

FIG 1. (**a**) SEM image of an as-fabricated nc-Si wire. The upper inset schematics illustrate the probing of the wires for electrical stress. The lower inset is a schematic cross section of the wire bridge over undercut SiO_2. The large area pads lie on SiO_2 and are in and out of the plane. **(b)** SEM image of an asymmetrically molten wire, 1.5 µm in length, after a 1 µs, 30 V pulse. **(c)** I-V characteristics for a 2.5 µm wire before and after the electrical contact between the tungsten probe and highly pulse. The linear I-V curves indicate the ohmic doped nc-Si.

Numerical modeling

Eq. (1) shows the 1D time dependent heat diffusion equation. The first term on the right hand side is the Fourier heat conduction due to the temperature gradient [7], and the second term is the Joule heat due to the constant current pulse. The third term represents heat conduction from the wire to the substrate through air and oxide following the approach described by Lin et al. [8]. The last term is the Thomson heat which is the thermoelectric heat exchanged between charge carriers and phonons when charge carriers travel along a temperature gradient [9]. In the case of heat conduction in conductors, phonons and free electrons moving randomly in the lattice conduct heat diffusively. In thermoelectric heating electrons forced to move in one direction by an electric field also transfer heat and modify the heat distribution in the material resulting in asymmetric heating. Thomson effect, a thermoelectric effect, arises in any material in the presence of electrical current and temperature gradient, and can be significant depending on the

magnitude of these and of Thomson coefficient, a thermoelectric property of the material related to the Seebeck coefficient by one of the Kelvin relations (Eq. 2).

$$\frac{dT}{dt} = \frac{1}{\rho_v C_v(T) A_x} \frac{d}{dx}(k(T) A_x \frac{dT}{dx}) + \frac{\rho(T) j_x^2}{\rho_v C_v(T)}$$
$$- \frac{1}{\rho_v C_v(T)} \frac{S}{G_u t_{wire}} (T - T_{subs}) - \frac{\beta(T)}{\rho_v C_v(T)} \vec{j}_x \cdot \nabla T \qquad (1)$$

$$\beta = T \frac{dS}{dT} = T\delta \qquad (2)$$

Thomson heat can be positive (emitted) or negative (absorbed) depending on the relative directions of the electric current and temperature gradient and the sign of the Thomson coefficient of the material, β [9]. The maximum temperature is shifted from the center by a certain amount referred to as Thomson shift. There is only limited experimental data on the temperature dependence of Seebeck coefficient of silicon, which determines the Thomson coefficient (Eq. 2). Fulkerson et al. measured the Seebeck coefficient of phosphorus doped polycrystalline silicon (poly-Si) with doping density of 12 ppm ($6x10^{17}$ cm^{-3}), and observed that Seebeck coefficient is negative, and its magnitude increases with temperature up to about 360 K, and decreases afterwards [10]. Gaidry's measurements on heavily phosphorus doped single crystal silicon show that the Seebeck coefficient is negative and has a minimum of -260 μV/K at approximately 600 K [11]. The Seebeck coefficient of phosphorus doped amorphous silicon (a-Si) with different conductivities, including highly doped, was measured by Jones et al. showing significantly larger Seebeck coefficient and dS/dT compared to heavily doped single-crystal or poly-Si and also a monotonous increase with temperature (Thomson coefficient always positive indicating that the transition temperature is probably below the temperature range studied) [12]. The peaked temperature dependence of Seebeck coefficient is expected for metals and semiconductors due to the phonon-drag effect. At low temperatures, high phonon-electron interaction results in phonon assisted electron diffusion (phonon-drag effect). Due to the phonon-drag effect the Seebeck coefficient increases in magnitude with increasing temperature up to a transition temperature T_{trans}. Above T_{trans}, the material is in the high temperature regime where phonon-phonon interaction dominates and electron-phonon interaction becomes negligible resulting in a decrease of the Seebeck coefficient magnitude with increasing temperature [9]. As a result of this peaked S(T), Thomson coefficient switches sign at T_{trans}. As seen in Eq. (1), for a given temperature gradient and current direction, the direction of the Thomson shift is determined by the sign of the Thomson coefficient. In this study the temperatures of interest is above room temperature. Since we don't have the Seebeck coefficient data for our films and there is no data in the literature for heavily doped nc-Si, in our simulations we use the data for two limit cases of heavily phosphorous doped poly-Si and heavily phosphorous doped a-Si, at high temperatures (both having positive Thomson coefficients). The numerical simulations are performed using two different Thomson coefficients β_1 and β_2, corresponding to δ_1=0.312 μVK^{-2} for the poly-Si [10] and δ_2=1.639 μVK^{-2} for the a-Si [12], where δ is the temperature coefficient of the Thomson coefficient (Eq. 2).

The large pads at each side of the wire are included in the 1D equation through a varying cross sectional area, A_x, corresponding to a varying current density. The initial and boundary

conditions are T(± (L/2+10 μm), t) = T(x, 0) = 300 K, where L is the length of the wire. The middle of the wire is located at x=0.

In Eq. (1), ρ_v is the density of silicon which is approximated as temperature independent, and it is equal to 2330 kgm^{-3} [13]. T and I are the temperature and the amplitude of current pulse, respectively. j_x ($j_x=I/A_x$) is the current density.

G_u represents the equivalent thermal conductivity of the heat path to the substrate which is equal to the serial combination of the thermal conductivity of SiO_2 and that of air. S and G_u are geometrical factors for a wire bridge [8]:

$$S = \frac{t_{wire}}{w_{wire}}\left(\frac{2t_{air}}{t_{wire}}+1\right)+1, \text{ and } \quad G_u = \frac{t_{air}}{k_{air}}+\frac{t_{ox}}{k_{ox}} \tag{3}$$

t_{wire}, t_{air} and t_{ox} are the thicknesses of the wire, air, and oxide layers, respectively. k_{air} and k_{ox} are the thermal conductivity of air and oxide, respectively. T_{subs} is the initial temperature of the substrate, which is room temperature (300 K).

In Eq. 1 k, C_v and ρ are the thermal conductivity, specific heat, and electrical resistivity, respectively. Since we don't have the material parameters for our films, for C_v, we used the data for the single crystal silicon given in [13] and for k we used the data pertaining to highly doped (10^{20} cm^{-3}) n-type poly-Si [14]. For the electrical resistivity ρ we assumed a linearly decreasing function of temperature. The temperature dependence of these material parameters is included in the model through the following approximate relations based on experimental data:

$$C_v(T) = C_{v0} + m(T - T_0) \tag{4a) [11]}$$

$$k(T) = \frac{1}{(-2.2\times10^{-11})T^3 + (9\times10^{-8})T^2 + (-1\times10^{-5})T + 0.014} \tag{4b) [12]}$$

$$\rho(T) = \rho_0 - \alpha(T - T_0) \tag{4c}$$

C_{v0}, the specific heat at room temperature (T_0 = 300 K), and m are 705 $Jkg^{-1}K^{-1}$ and 0.2 $Jkg^{-1}K^{-2}$, respectively (Eq. 4a) [13]. The thermal conductivity at room temperature is 60 $Wm^{-1}K^{-1}$ [14]. ρ_0 is the room-temperature resistivity of the film measured by four-point probe measurement technique ($\rho_0=3\times10^{-4}$ Ω.m). From current monitoring during the constant voltage pulse, I(t), it is observed that resistivity drops to ~ 3×10^{-5} Ω.m at just below melting temperature (1687 K). From the known resistivity values at room temperature and at melting temperature, α=1.681 Ω.m/K is obtained [Eq. (4c)].

Eq. (1) is solved numerically with the given material parameters to obtain the temperature profile on the electrically pulsed wires.

Results and discussion

Figure 2 shows the temperature distribution for a wire 1.5 μm long, 300 nm wide and 80 nm thick, obtained from the solution of Eq. (1) with and without Thomson heat term for a 1μs, 350 μA current pulse in +x direction. The effect of Thomson heat is calculated for two Thomson coefficients β_1 and β_2 as indicated above. When Thomson effect is not taken into account the maximum temperature occurs at the center of the wire. The addition of Thomson heat results in a shift of the peak towards the negative terminal end (for positive Thomson coefficient), and the shift is more significant for the larger Thomson coefficient (with all other parameters the same).

Due to Joule heating, the temperature gradient and the current are in the same direction in the left half of the wire, and in opposite direction in the right half. Therefore, Thomson heat is absorbed in one half, and evolved in the other half, resulting in an asymmetric temperature profile.

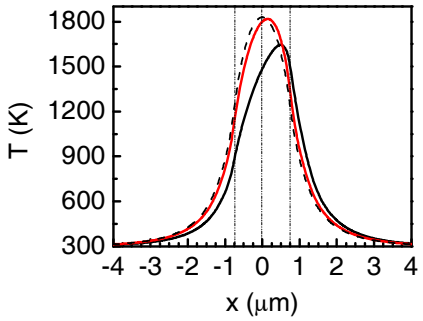

FIG 2. Temperature distributions obtained from numerical modeling, on a wire 1.5 μm long, 300 nm wide and 80 nm thick, with Thomson effect (solid lines) and without Thomson effect (dashed line) after electrically stressed by 1 μs 350 μA pulse (snapshots at t=1 μs). Large contact pads extend from -10.75 μm to -0.75 μm on left, and from 0.75 μm to 10.75 μm on right. Wire is located between x=-0.75 μm and x=0.75 μm. For red solid curve δ=0.312 μVK^{-2} and the corresponding shift is 0.15 μm. For black solid curve δ=1.639 μVK^{-2} and the corresponding shift is 0.49 μm.

Figure 3(a) shows the time evolution of the temperature distribution during electrical stress of 350 μA, up to 1 μs, for δ=1.639 μVK^{-2}. At t=50 ns, temperature peak is located at x=0.22 μm; the shift increases with time and reaches 0.49 μm at t=1 μs. The cooling process after the termination of the 1 μs, 350 μA pulse is shown in Figure 3(b). The highest curve is the profile at the end of the pulse, at t=1 μs, and the lowest curve is the profile when t=1.175 μs. For this example, after 175 ns the whole wire cools down to room temperature. As cooling proceeds the temperature peak moves towards the middle of the wire since there is no asymmetry introduced by the electrical current.

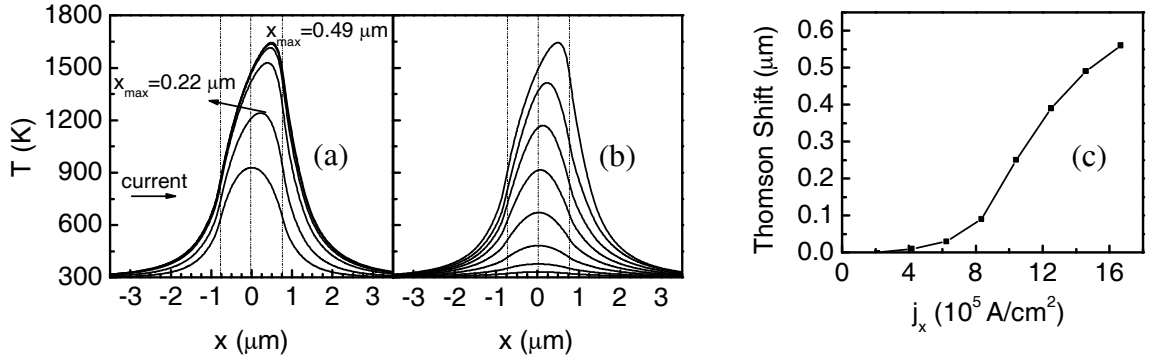

FIG 3. Temperature profiles obtained from numerical modeling on a wire 1.5 μm long, 300 nm wide, and 80 nm thick. **(a)** Time evolution of the temperature profiles during electrical stress of 350 μA. From the lowest curve to the highest one, t = 25 ns, 50 ns, 100 ns, 150 ns, 200 ns and 1 μs. Steady state is reached at t ~ 200 ns. **(b)** Cooling process of the wire in 25 ns increments from t=1 μs (end of the 350 μA pulse) to t=1.175 μs. **(c)**Thomson shift versus current density for the same wire dimensions, with δ=1.639 μVK^{-2}.

Figure 3(c) shows the Thomson shift as a function of electrical current density for the same wire dimensions. Increasing current density causes increased Joule heating and therefore a steeper temperature profile along the wire. Both larger current density and larger temperature gradient result in increased Thomson heat (Eq. 1) which causes a larger Thomson shift.

The modeling results show significant Thomson shifts in qualitative agreement with the experimental observations. In the experiments, the current densities at which the partial melting initiates is on the order of 10^7 A/cm^2. In the numerical calculations the melting temperature is reached when the current density is on the order of 10^6 A/cm^2. Because the present model does not include solid-liquid phase change, the current density is kept lower than the experimental

values so that the wire temperature does not increase beyond melting temperature. Higher current densities are expected to result in larger Thomson shifts [Fig. 3(c)]. In order to accurately simulate the Thomson effect on Joule heated wires the solid-liquid phase change has to be included in the model, as well as the experimental data for the electrical, thermal and thermoelectric properties of the films from which the wires are made.

Summary

Our experimental observations of silicon wires electrically stressed with high voltage and high current show that Thomson effect (thermoelectric heat in a uniform material when an electrical current passes along a temperature gradient) plays a significant role in the heat transport in these structures and results in a significant distortion of the temperature profile along the wires. Numerical modeling based on limited experimental data shows qualitative agreement with the experimental observations. Our results indicate that Thomson effect should be considered in small scale devices that operate under high current densities.

Acknowledgements

The devices were fabricated at the Cornell Nanoscale Science and Technology Facility. The authors would like to thank Rauf Gungor, with the Department of Chemical Engineering, University of Massachusetts at Amherst, and Eric Pop, with the Department of Electrical and Computer Engineering, University of Illinois at Urbana Campaign, for valuable discussions.

References

1. G. Chen, A. Shakouri, J. Heat Trans. 124, 242 (2002).
2. M. J. Huang, R. H. Yen, and A. B. Wang, International Journal of Heat and Mass Transfer 48, 413 (2005).
3. A. Pirovano, A. L. Lacaita, A. Benvenuti, F. Pellizzer, R. Bez, IEEE Trans. Elect. Dev. 51, 452 (2004).
4. E. Pop, S. Sinha and K. E. Goodson, Proceedings of the IEEE 94, 1587 (2006).
5. C. H. Mastrangelo, J. H. Yeh, R. S. Muller, IEEE Trans. Elect. Dev. 39, 1363 (1992)
6. A. Jungen, M. Pfenninger, M. Tonteling, C. Stampfer, C. Hierold, J. Micromech. Microeng. 16, 1633 (2006)
7. L. C. Thomas, *Heat Transfer Professional Version* (Prentice Hall, Inc, New Jersey, 1993).
8. L. Lin, M. Chiao, Sens. Actuators A 55, 35 (1996).
9. D. K. C. MacDonald, *Thermoelectricity: an Introduction to the Principles* (Dover Publications Inc., Mineola, NY, 2006) P. 9-24.
10. W. Fulkerson, J. P. Moore, R. K. Williams, R. S. Graves, D. L. McElroy, Phys. Rew. 167, 765 (1968).
11. T. H. T. Gaidry, "Thermal Conductivity, Seebeck Coefficient, and Electrical Resistivity of Heavily Phosphorous-Doped Silicon from 313 K to 673 K," Technical Report, South Dakota School of Mines and Technology Rapid City, Department of Physics, available from the National Technical Information Service, (1967).
12. D. I. Jones, P. G. Le Comber, W. E. Spear, Phil. Mag. 36, 541 (1977)
13. Y. S. Touloukian, *Thermophysical Properties of High Temperature Solid Materials* (The Macmillan Company NY, 1967).
14. C. D. Lott, T. W. McLain, J. N. Harb, and L. L. Howell, Sens. Actuators A 101, 239 (2002).